

Supporting Information for:
**Cs₂InAgCl₆: A New Lead-Free Halide Double
Perovskite With Direct Band Gap**

George Volonakis,[†] Amir Abbas Haghighirad,[‡] Rebecca L. Milot,[‡] Weng H. Sio,[†]
Marina R. Filip,[†] Bernard Wenger,[‡] Michael B. Johnston,[‡] Laura M. Herz,[‡]
Henry J. Snaith,[‡] and Feliciano Giustino^{*,†}

[†]*Department of Materials, University of Oxford, Parks Road OX1 3PH, Oxford, UK*

[‡]*Department of Physics, Clarendon Laboratory, University of Oxford, Parks Road, Oxford
OX1 3PU, United Kingdom*

E-mail: feliciano.giustino@materials.ox.ac.uk

Phone: (+44) 01865 272380

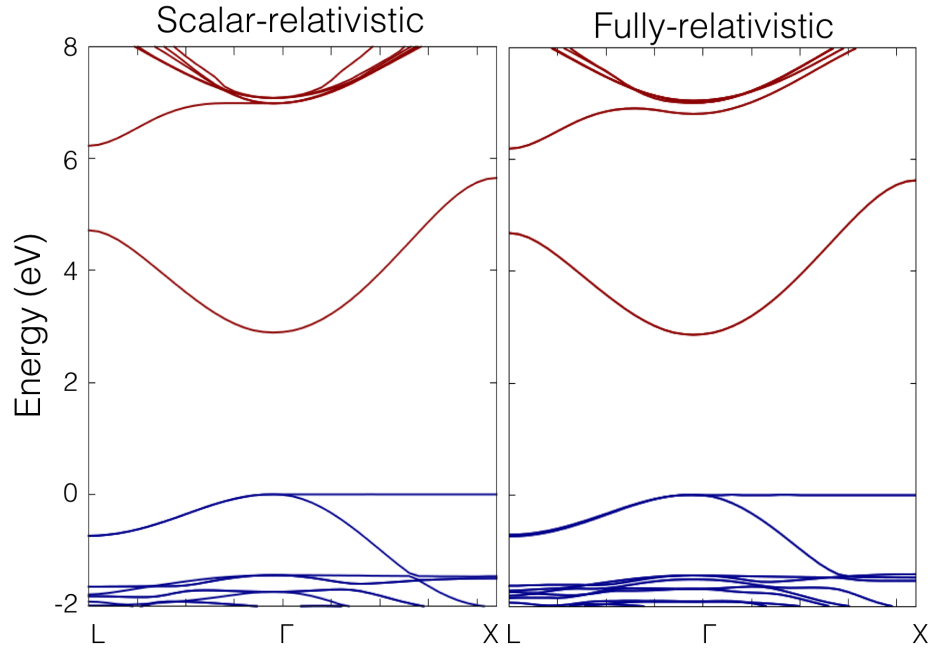


Figure S1: Effect of spin-orbit coupling in the band structure of $\text{Cs}_2\text{InAgCl}_6$: (a) Scalar-relativistic and (b) fully-relativistic band structure calculated using the PBE0 hybrid functional. The zero of energy is set to the top of the valence band. The two band structures are practically indistinguishable.

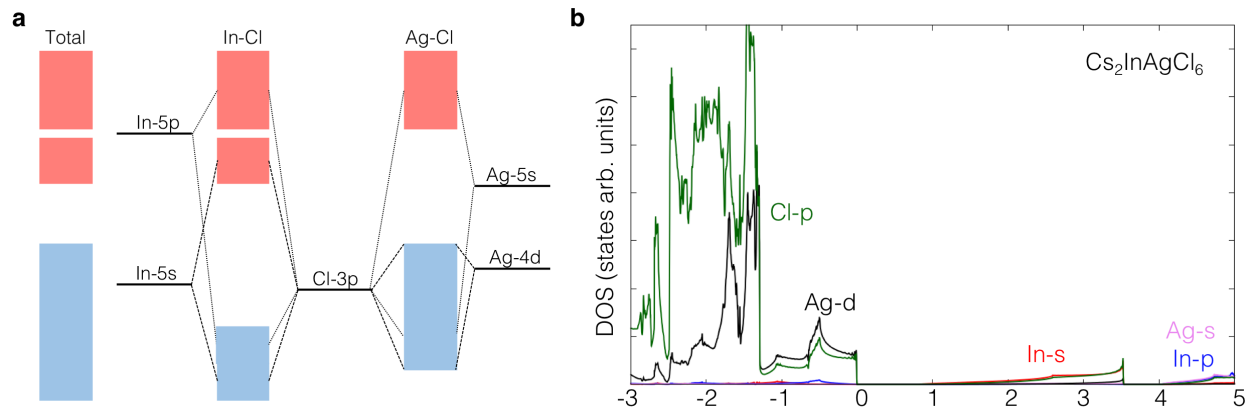


Figure S2: Molecular orbital diagram and partial density of states of $\text{Cs}_2\text{InAgCl}_6$: (a) Qualitative molecular orbital diagram of $\text{Cs}_2\text{InAgCl}_6$, as extracted from the projected density of states. The thick black lines indicate atomic one-electron energies (www.nist.gov), blue and red rectangles indicate occupied and unoccupied states, respectively. We used the Cs-5s level as the common energy reference. (b) Partial DOS of $\text{Cs}_2\text{InAgCl}_6$ within DFT/LDA, with the zero of energy set to the valence band top. The labels indicate the dominant orbital character in each case.

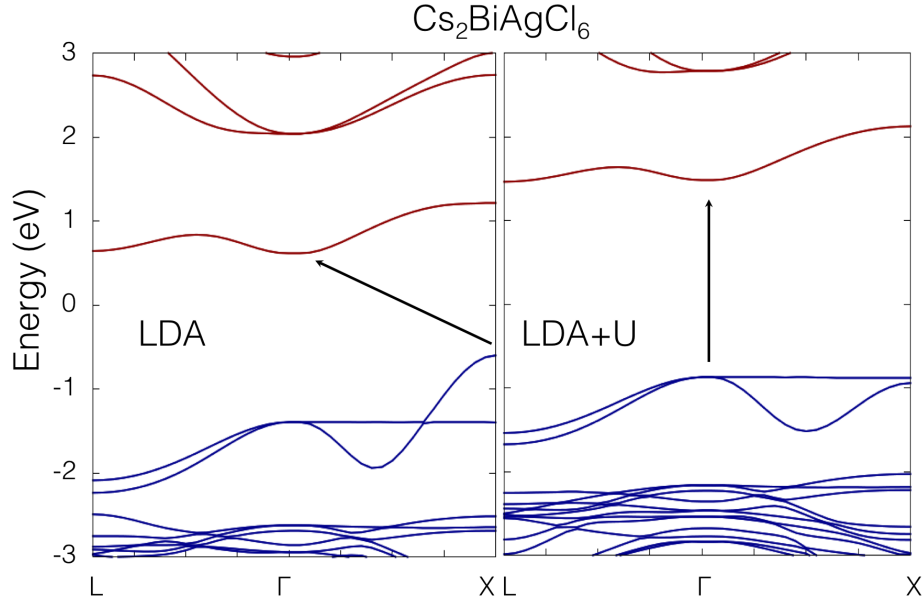


Figure S3: Origin of indirect band gap of $\text{Cs}_2\text{BiAgCl}_6$: In the Bi/Ag halide elpasolite $\text{Cs}_2\text{BiAgCl}_6$ the Bi s states at the top of the valence band interact with the directional Ag d states along the $[100]$ direction; this interaction pushes the valence band top to the X point and leads to an indirect band gap in $\text{Cs}_2\text{BiAgCl}_6$. In this figure we show that, by artificially removing the Bi s states from the top of the valence band, the band gap becomes direct at Γ . The left panel shows a standard DFT/LDA calculation of $\text{Cs}_2\text{BiAgCl}_6$; here the top of the valence band is at X and the band gap is indirect. The right panel shows a DFT+ U calculation with a fictitious Hubbard parameter $U = 10$ eV on the Bi- s orbitals; here the top of the valence band is at Γ and the gap is direct.

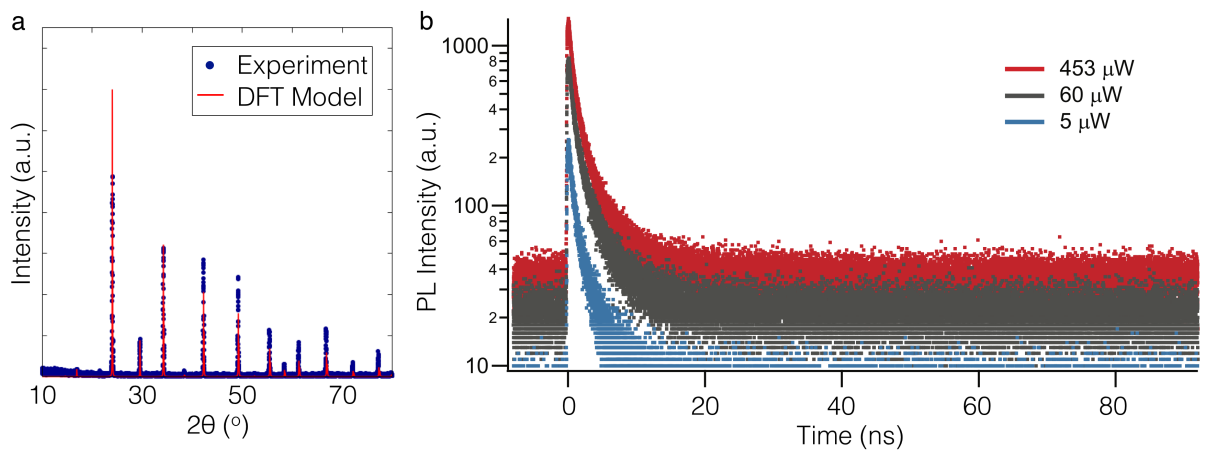


Figure S4: Additional characterization of $\text{Cs}_2\text{InAgCl}_6$: (a) Powder XRD pattern measured for the as-synthesized $\text{Cs}_2\text{InAgCl}_6$ (blue dots), and pattern calculated from the atomistic model in Figure 1a, after optimizing the structure using the measured lattice constant $a = 10.47 \text{ \AA}$. (b) Dependence of the time-resolved PL intensity upon the pump power.

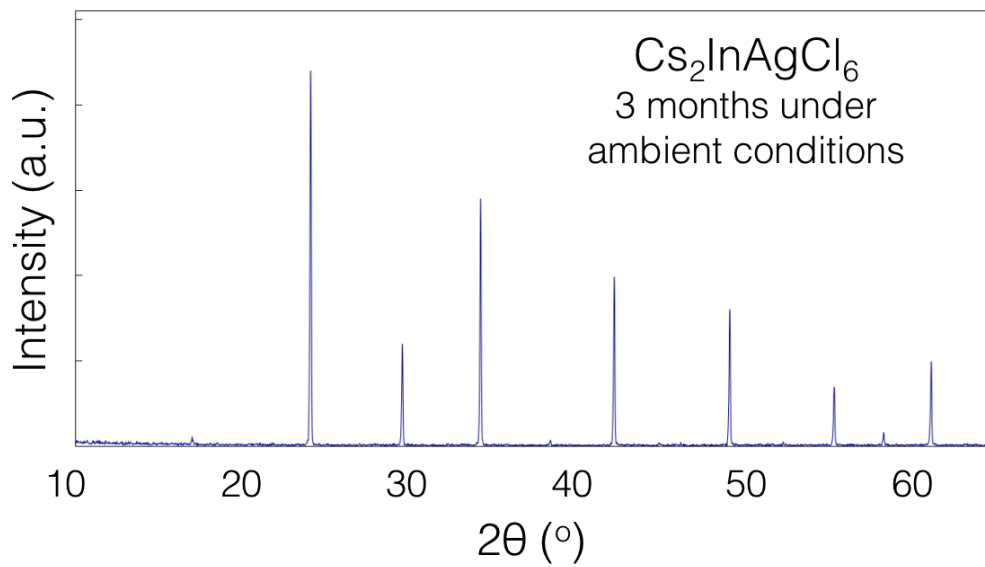


Figure S5: Structural stability of $\text{Cs}_2\text{InAgCl}_6$: Measured X-ray diffraction (XRD) pattern for $\text{Cs}_2\text{InAgCl}_6$ after three months in ambient conditions.

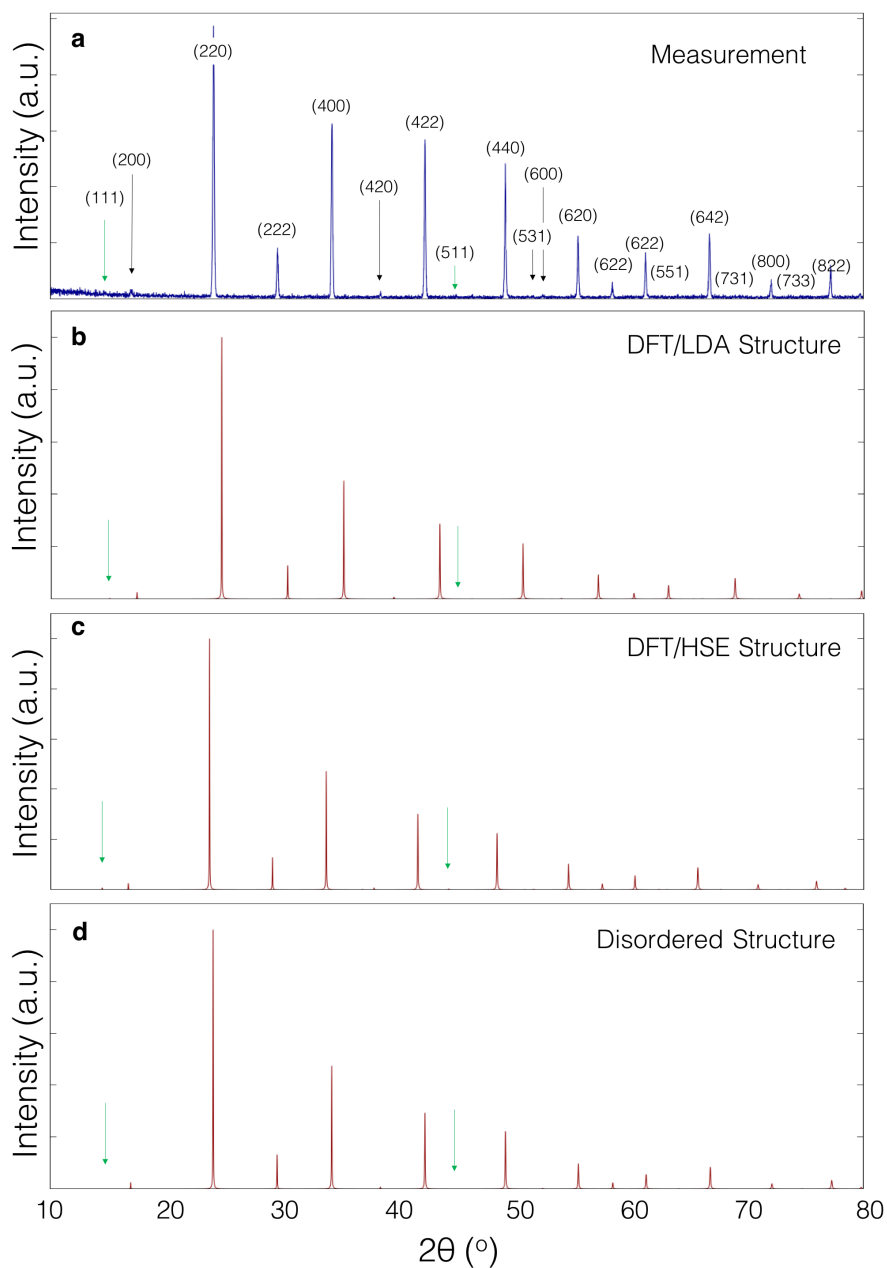


Figure S6: Cation ordering in $\text{Cs}_2\text{InAgCl}_6$: (a) Measured X-ray diffraction (XRD) pattern for $\text{Cs}_2\text{InAgCl}_6$. (b) Calculated XRD pattern for the theoretical fully-ordered structure, optimized within DFT/LDA. (c) As in (b), but optimized using DFT/HSE. (d) Calculated XRD pattern for a fully-disordered model of $\text{Cs}_2\text{InAgCl}_6$. In all panels the green arrows indicate the peaks that are associated with cation ordering effects.

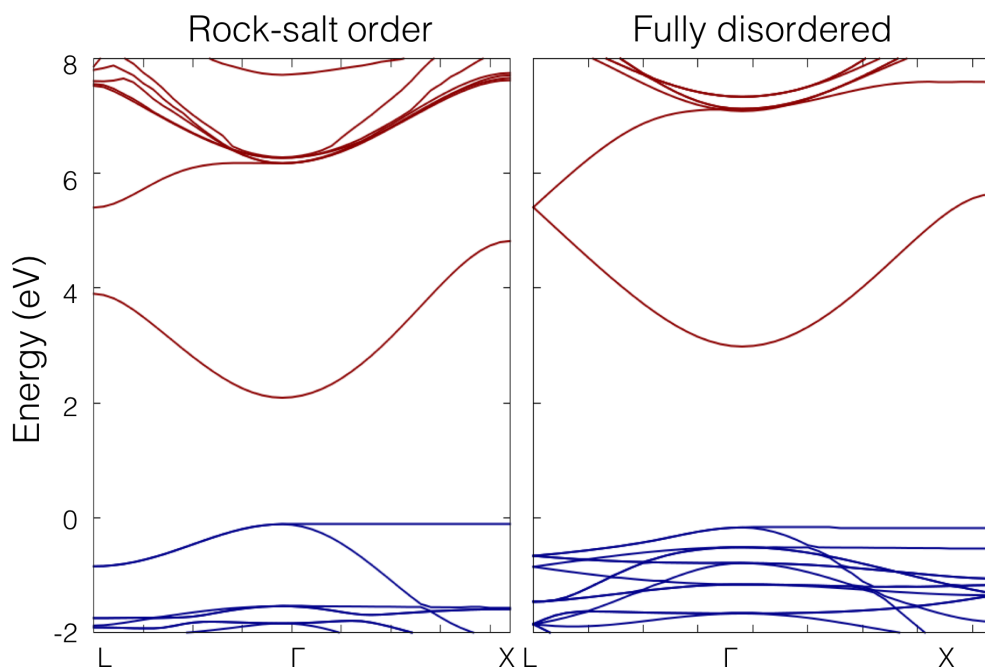


Figure S7: Effect of cation ordering on the band structure of $\text{Cs}_2\text{InAgCl}_6$: Band structure of $\text{Cs}_2\text{InAgCl}_6$ calculated within DFT/HSE for two models: elpasolite structure with Ag and In in rock-salt order (left), and perovskite structure (in the elpasolite unit cell) with In and Ag replaced by a virtual atom $0.5 \text{ Ag} + 0.5 \text{ In}$. For the virtual atom we used Cd which lies precisely between Ag and In in the Periodic Table. In both cases the lattice constant was set to the experimental value.

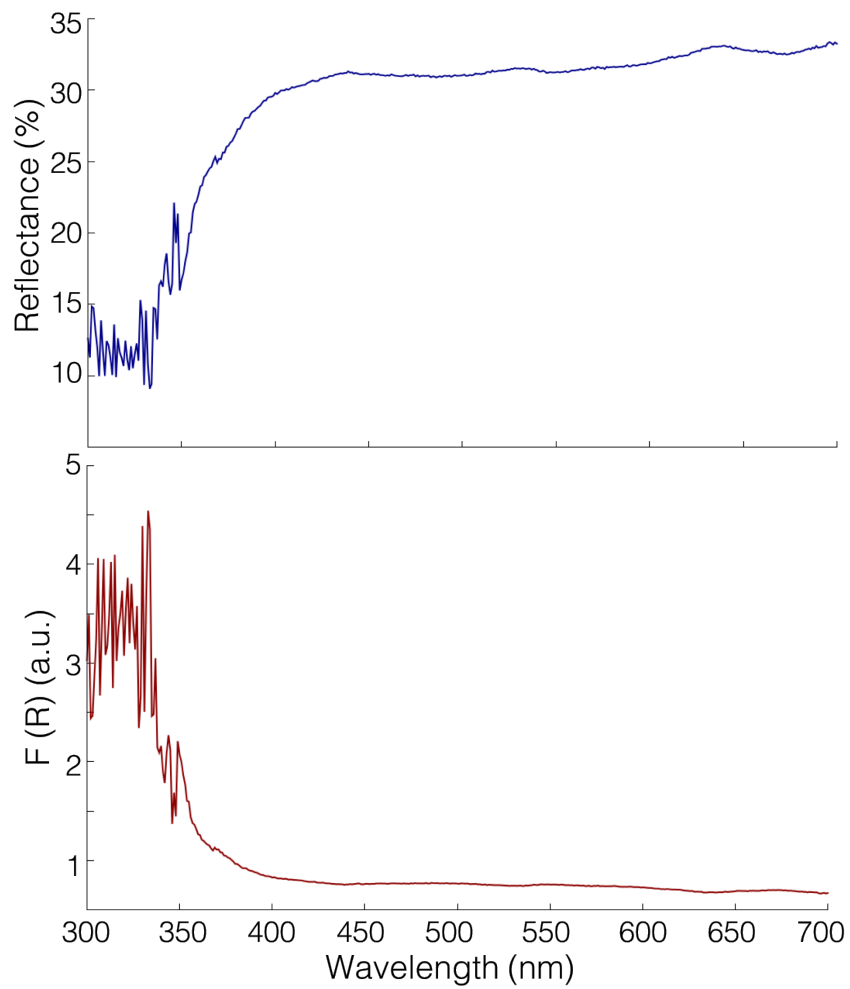


Figure S8: Measured optical properties of $\text{Cs}_2\text{InAgCl}_6$: Reflectance and Kubelka-Munk function measured using an integrating sphere for $\text{Cs}_2\text{InAgCl}_6$.

Table S1: DFT structural parameters and electronic band gaps: Lattice constant, bond lengths and electronic band gaps (E_g) of $\text{Cs}_2\text{InAgCl}_6$ calculated within HSE and PBE0, by employing LDA, PBE, and HSE for the structural optimization.

| Structural optimization functional | Lattice constant (\AA) | In-Cl bond length (\AA) | Ag-Cl bond length (\AA) | E_g HSE (eV) | E_g PBE0 (eV) |
|------------------------------------|-----------------------------------|------------------------------------|------------------------------------|----------------|-----------------|
| LDA | 10.20 | 2.50 | 2.59 | 2.1 | 2.9 |
| PBE | 10.65 | 2.57 | 2.76 | 2.4 | 3.0 |
| HSE | 10.62 | 2.54 | 2.77 | 2.6 | 3.3 |

Table S2: Rietveld refinement of Cs₂InAgCl₆: Refined structural parameters obtained from Rietveld refinement, assuming an elpasolite structure (with Ag and In arranged in a rock-salt sublattice).

| | |
|-------------------------|-------------------------------------|
| Compound | Cs ₂ InAgCl ₆ |
| Measurement temperature | 293 K |
| Crystal system | Cubic |
| Space group | $Fm\bar{3}m$ |
| Unit cell dimensions | a = 10.467 (1) Å α = β = γ = 90° |
| Volume | 1147.01 Å ³ |
| Z | 4 |
| Density (calculated) | 4.064 g/cm ³ |
| Number of data | 10449 |
| Wavelength | 1.5405 Å |

| Atomic Wyckoff-positions | Atom | Site | x | y | z | site occupancy |
|--------------------------|------|------|--------|------|------|----------------|
| | Cs | 8c | 0.25 | 0.25 | 0.25 | 1 |
| | In | 4a | 0 | 0 | 0 | 1 |
| | Ag | 4b | 0.5 | 0.5 | 0.5 | 1 |
| | Cl | 24e | 0.2275 | 0 | 0 | 1 |